PHYSICAL REVIEW A **96**, 063827 (2017)

Frequency dependence of coherently amplified two-photon emission from hydrogen molecules

Hideaki Hara,[1,*] Yuki Miyamoto,[1] Takahiro Hiraki,[1] Takahiko Masuda,[1] Noboru Sasao,[1] Satoshi Uetake,[1,2] Akihiro Yoshimi,[1] Koji Yoshimura,[1] and Motohiko Yoshimura[1]

[1]*Research Institute for Interdisciplinary Science, Okayama University, Okayama 700-8530, Japan*

[2]*PRESTO, Japan Science and Technology, Okayama 700-8530, Japan*

(Received 9 June 2017; published 19 December 2017)

We investigate how the efficiency of coherently amplified two-photon emission depends on the frequency of one of the two emitted photons, namely the signal photon. This is done over the wavelength range of 5.048–10.21 μm by using the vibrational transition of parahydrogen. The efficiency increases with the frequency of the signal photon. Considering experimental errors, our results are consistent with the theoretical prediction for the present experimental conditions. This study is an experimental demonstration of the frequency dependence of coherently amplified two-photon emission, and also presents its potential as a light source.

DOI: 10.1103/PhysRevA.96.063827

I. INTRODUCTION

Coherence among an ensemble of atoms or molecules interacting with photons plays a significant role in atomic, molecular, and optical physics. It gives rise to many interesting phenomena that are not observed in ensembles of incoherent atoms or molecules, for example, electromagnetically induced transparency [1], stimulated Raman adiabatic passage [2], photon echo [3], and superradiance [4]. Coherent amplification of rare processes is one of the uses of the coherence among ensembles of particles. For example, a superradiant laser using an optical clock transition has been proposed as a way to improve the stability of today's best clocks [5]. Coherent amplification can also be used to observe extremely rare deexcitation processes in atoms or molecules that emit neutrinos and a photon, by which the important parameters of neutrinos, such as their absolute masses, mass type, and CP-violating phases, can be determined [6].

One such rare process is two-photon emission (TPE), which is especially important in atomic physics, astrophysics, and nuclear physics [7–12]. As the most basic multiphoton emission process, it is therefore appropriate to use TPE to study the coherent amplification of rare processes.

Harris and Jain have studied coherently amplified TPE theoretically [13]. They proposed that Pb vapor could be used as the medium for an optical parametric oscillator with broad gain bandwidth. This process is similar to what we refer to as coherently amplified TPE. Although Harris and Jain provided a theoretical equation for TPE efficiency based on the Maxwell-Bloch equations, no experimental data have been reported as yet.

Recently, we succeeded in coherently amplifying the TPE process from the first vibrationally excited state of the electronic ground state ($X\,^1\Sigma_g^+$) of parahydrogen molecules (p-H_2) [14,15], the energy diagram of which is shown in Fig. 1. This transition in p-H_2 is suitable for observing TPE. This is because single-photon $E1$ transitions between vibrational levels of homonuclear molecules are forbidden in the selection rules, but two-photon $E1 \times E1$ transitions are allowed. The TPE, whose spontaneous emission rate is 7×10^{-12} Hz for p-H_2, was enhanced by coherence provided by stimulated Raman scattering and a trigger provided by midinfrared laser pulses. The sum of the frequency $\omega_{\rm trig}$ of the trigger pulses and the frequency $\omega_{\rm sig}$ of the TPE signal is equal to the difference between the vibrational frequency $\omega_{\text{p-H}_2}$ of the p-H_2, which corresponds to a wavelength of 2403 nm, and the two-photon detuning δ. We also measured the dependence of the TPE rate on the energy and timing of the trigger pulses and found that the observed behaviors were consistent with a simulation using the Maxwell-Bloch equations.

In our previous paper [15], we fixed the frequency of the trigger pulse at roughly half the energy difference of the vibrational levels. In the present paper, in contrast, we vary the frequency of the TPE signal by changing the frequency of the trigger pulses. Harris and Jain predicted the dependence of TPE on the signal frequency theoretically [13]. The present paper reports measurements of the frequency dependence of coherently amplified TPE over the wavelength range of 5.048–10.21 μm, and also presents an optical generation procedure that differs from ordinary optical parametric processes in nonlinear crystals.

II. EXPERIMENTAL SETUP

Figure 2 shows the experimental setup, which is a modification of one described previously [15]. In the present experiment, the frequency of the trigger field can be tuned.

The p-H_2 gas is prepared by converting normal hydrogen gas in a magnetic catalyst Fe(OH)O that is cooled to roughly 14 K by a Gifford-McMahon refrigerator. The prepared p-H_2 gas is enclosed within a copper cell with a diameter of 20 mm and a length of 150 mm. The temperature of the cell is kept at 78 K in a cryostat, at which temperature almost all the p-H_2 molecules exist in the ground state. The pressure of the p-H_2 is fixed at 60 kPa, which corresponds to a density of 5.6×10^{19} cm^{-3}. In addition to narrow Doppler broadening due to the low temperature, the decoherence time of the vibrational level of p-H_2 has its maximum in this pressure region thanks to Dicke narrowing [16]. The decoherence time estimated from the reported Raman linewidth [16] is roughly 2.4 ns. The input sides of the cell and the cryostat are sealed with magnesium fluoride (MgF_2) windows. With consideration

*hhara@okayama-u.ac.jp

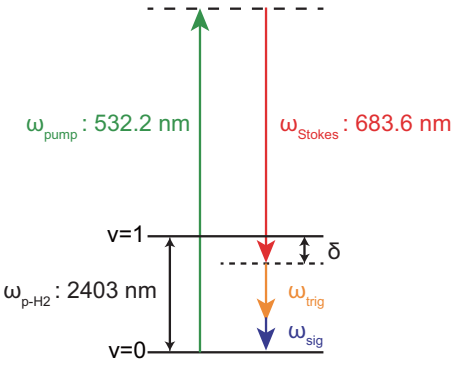

FIG. 1. Energy diagram of p-H_2. The energy difference between the $v = 0$ and $v = 1$ states corresponds to a wavelength of 2403 nm. The 532.2 nm and 683.6 nm pulses are used for the Raman transition. The two-photon detuning δ can be shifted by changing the wavelength of the 683.6 nm pulses. ω_{trig} is the frequency of the trigger pulses for TPE. ω_{sig} is the frequency of the TPE signal.

for the wavelength-dependent transmittance, the output sides are sealed with either other MgF_2 windows for $\lambda_{\text{sig}} < 7\ \mu$m or barium fluoride ($BaF_2$) windows for $\lambda_{\text{sig}} > 7\ \mu$m.

Coherence between the vibrational states is prepared by Raman transitions. To generate high coherence, lasers with high intensity and narrow linewidth are required. We use $\lambda = 532.2$ nm as a pump laser pulse (ω_{pump}) and $\lambda = 683.6$ nm as a Stokes laser pulse (ω_{Stokes}). We refer to these two visible pulses as driving fields. The 532.2 nm pulses are second harmonics of an injection-seeded Nd:YAG laser. The repetition rate, the duration (FWHM), and the linewidth (FWHM) of these pulses are 10 Hz, 8 ns, and 100 MHz, respectively. A portion of the 532.2 nm pulses is used to generate the 683.6 nm pulses via optical parametric generation and amplification. In this process, a continuous-wave external-cavity diode laser is used for injection seeding to control the wavelength of the 683.6 nm pulses and narrow their linewidth. The duration and the linewidth range of the 683.6 nm pulses are 6 ns and 150–250 MHz, respectively. Because both driving pulses originate from the same laser, the timing jitter between them is negligible. The input energies of the 532.2 nm and 683.6 nm pulses at the input window are roughly 15 mJ/pulse and 3.5 mJ/pulse, respectively. The energy difference between these two pulses is nearly equal to the vibrational energy of p-H_2. Two-photon detuning δ from resonance, defined as $\delta = \omega_{\text{p-H}_2} - (\omega_{\text{pump}} - \omega_{\text{Stokes}})$, can be tuned within several GHz by changing the wavelength of the 683.6 nm pulses. The detuning uncertainty is ± 170 MHz as estimated from the absolute accuracy of ± 75 MHz of the wave meter. The detuning δ is adjusted to maximize the TPE signal energy, and ranges from -70 MHz to $+130$ MHz. Within the uncertainty, the TPE signal is maximum at resonance. We maximize the signal and therefore δ is treated as zero in the following sections.

The TPE is triggered by midinfrared pulses, which we refer to here as the trigger field. The detailed laser setup is described in Ref. [17]. The trigger pulses are generated by using optical parametric generation and amplification, and different frequency generation. The repetition rate and the duration of the trigger pulses are 10 Hz and 2 ns, respectively. The trigger pulses originate from another injection-seeded Nd:YAG laser ($\lambda = 1065$ nm, $\omega_{\text{Nd:YAG}}$). To control the wavelength of the trigger pulses, a continuous-wave Ti:sapphire laser ($\omega_{\text{Ti:S}}$) is used for injection seeding. The frequency of the trigger pulses, as an output of nonlinear optical processes, is $\omega_{\text{trig}} = \omega_{\text{Ti:S}} - \omega_{\text{Nd:YAG}}$. The wavelength of the trigger pulses is tuned from 3143 nm to 4587 nm by changing the wavelength of the Ti:sapphire laser from 795.2 nm to 864.0 nm. We confirm the wavelength of the generated trigger pulses by measuring their spectra with a monochromator. The input energies of the trigger pulses are several hundred microjoules per pulse.

The driving and trigger fields are superposed by dichroic mirrors, collinearly aligned, and then injected into the p-H_2 target cell with polarizations that are parallel to each other. The mutual timing between the driving and trigger fields is adjusted to maximize the TPE signal energy. The driving pulses are nearly collimated at the target cell. The beam diameters, defined by D4σs, are 2.5 mm for the 532.2 nm pulses and 1.6 mm for the 683.6 nm pulses. The trigger pulses are loosely focused at the center of the target cell. Their D4σ is 1.0 mm at the center of the cell and 1.4 mm at the end of the cell. It is possible to increase the TPE signal intensity by focusing the laser fields. However, the divergence angle of the generated TPE signal pulses increases because of the small beam waist. This effect is more pronounced for longer wavelengths. Hence, to avoid part of the TPE signal not reaching the detectors, we use nearly collimated beams.

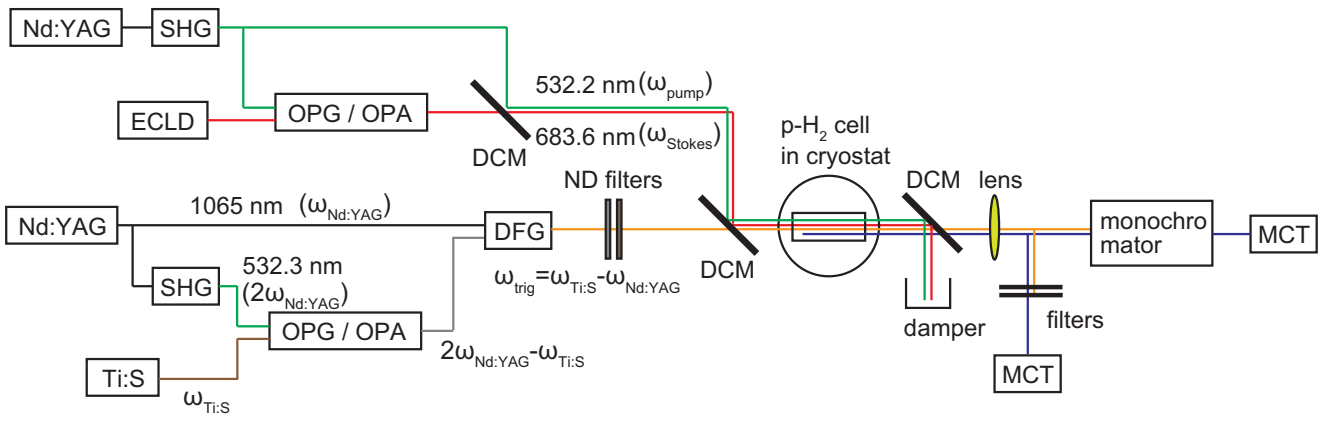

FIG. 2. Experimental setup.

If coherence is prepared, the trigger photons induce the coherently amplified TPE process, which generates pairs of another trigger photon and a TPE signal photon. The TPE signal energy is measured by a mercury-cadmium-telluride (MCT) midinfrared detector. Besides the paired photons, higher-order Raman-scattering pulses, residual driving pulses, and trigger pulses come out from the p-H_2 cell. By being separated from the other undesired photons by a dichroic mirror and optical filters, only the TPE signal photons reach the detector. Furthermore, at several trigger wavelengths, we observe the spectrum of the TPE signal by means of the monochromator and another MCT detector to confirm that the observed signals originate from TPE.

III. RESULTS

Figure 3(a) shows an example of the observed spectrum of the TPE signal. In this case, the wavelength of the trigger field is set to 4423 nm and the center wavelength of the observed TPE signal is 5262 nm. The latter is consistent with the value of 5263 nm that is expected from energy conservation ($\omega_{\mathrm{trig}} + \omega_{\mathrm{sig}} = \omega_{\mathrm{p\text{-}H_2}}$). We attribute the deviation of 1 nm to the uncertainty of the monochromator. The data points in Fig. 3(b) indicate the center wavelengths of the observed TPE signal at various trigger wavelengths. The red line is obtained from energy conservation. These results confirm that the photons

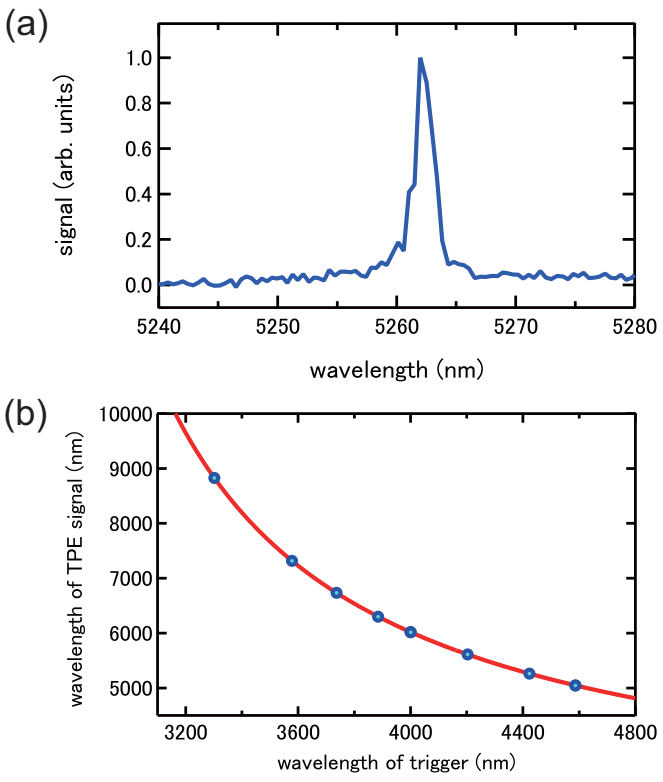

FIG. 3. (a) Example of a measured TPE signal spectrum. The wavelength of the trigger field is 4423 nm, and the center wavelength of the TPE signal is 5262 nm. (b) The blue circles indicate the center wavelengths of TPE signal spectra measured at various trigger wavelengths. The red line indicates the calculated variation.

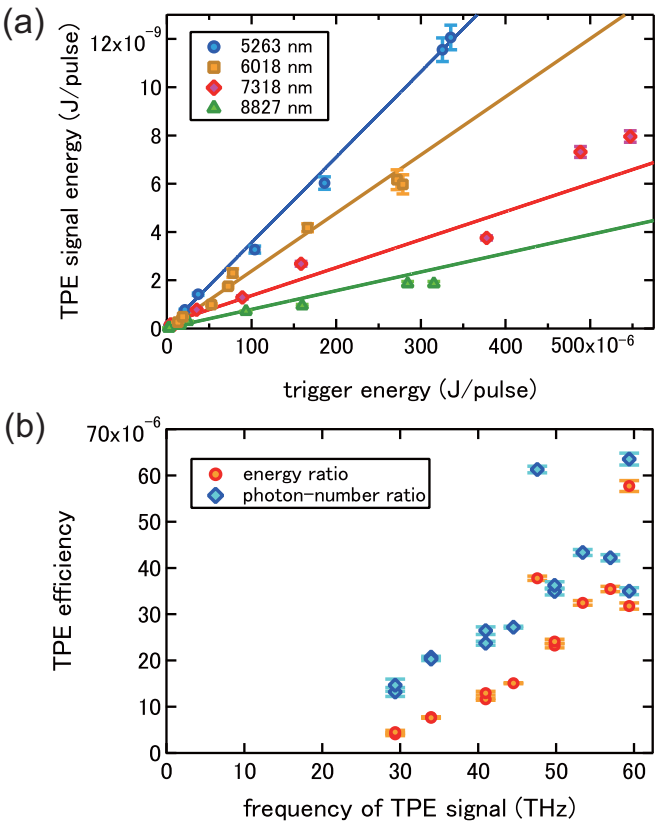

FIG. 4. (a) Examples of measured TPE signal energies for various trigger energies. The blue circles, orange squares, red diamonds, and green triangles represent the data for (λ_{trig},λ_{sig}) = (4423,5263) nm, (4001,6018) nm, (3578,7318) nm, and (3302,8827) nm, respectively. The error bars indicate standard errors. The solid lines are linear fits to the data. (b) TPE efficiency. The orange circles represent efficiency as defined by the energy ratio of the TPE signal to the trigger at each TPE signal frequency. They correspond to the slopes determined by the linear fits in (a). Each error bar indicates 1σ of the slope of the linear fit. The blue diamonds represent efficiency as defined by the photon-number ratio of the TPE signal pulse to the trigger pulse.

observed in this wide frequency range are generated from TPE. We cannot measure the TPE signal spectrum for wavelengths longer than 10 μm because the spectral amplitudes are too small.

We investigate the TPE efficiency for various frequencies of the TPE signals. The TPE efficiency can be defined either as the ratio of the TPE signal energy to the trigger energy or as the ratio of the number of photons in the TPE signal pulse to that in the trigger pulse. We measure the TPE signal energies at several trigger-pulse energies while changing the wavelength of the trigger field. We use neutral density filters to change the trigger-pulse energy at each wavelength. Each input trigger energy is measured by energy meters just in front of the cryostat and the actual trigger energy in the target cell is estimated by correcting the measured one for the transmittance of the input windows. The actual TPE signal energy is estimated from the TPE signal intensity measured by the MCT detector, accounting for the transmittance of the optics. Figure 4(a) shows examples of the measured

dependence of TPE signal energy on trigger energy. Each data point represents a pulse energy averaged over 200 pulses. The measured dependence for each wavelength is represented by a linear function; this was behavior that we have observed previously [15]. It is consistent with a simulation using the Maxwell-Bloch equations in the case of low trigger energy. The equations we use for the simulation are shown in Ref. [14]. The solid lines in Fig. 4(a) are linear fits to the data. The linear functions have nonzero intercepts to eliminate any background effect. The slopes correspond to the TPE efficiency. The intercepts range from -0.04 nJ/pulse to $+0.2$ nJ/pulse, which are small compared with the measured TPE signal energies and hence can be neglected.

The data points in Fig. 4(b) represent the TPE efficiency as defined by the ratio of energies and by the ratio of photon numbers, as a function of the frequency of the TPE signal. The frequency range of the observed TPE signals is 29–59 THz, which corresponds in wavelength to an infrared range of 5.048–10.21 μm. At several frequencies, the data are measured twice to confirm the reproducibility. It is difficult to observe TPE signal pulses of frequencies below 25 THz with the current output windows and detectors. The efficiency tends to increase with the frequency of the TPE signal. Even if the TPE rate does not change, the TPE efficiency defined by the ratio of energies increases because $\hbar\omega_{\rm sig}/\hbar\omega_{\rm trig}$ increases. However, the fact that the TPE efficiency as defined by the ratio of photon numbers also increases indicates that the TPE rate itself increases. We consider the fluctuations of the data points to be due to instability of the experimental setup. The prepared coherence has finite fluctuations. Indeed, the measured energy of the fourth Stokes scattering significantly varies at each point. The relative standard deviation of it is 70%. It is sensitive to coherence amplitude because it is a higher-order Raman process. Therefore, the fluctuation of the prepared coherence ($|\rho_{ge}|$) can be estimated from the fluctuation of the energy of the fourth Stokes scattering ($E_{\rm St4}$). We run the numerical simulation of the Maxwell-Bloch equations for the present experimental conditions. If the energy of the pump laser pulses ($E_{\rm pump}$) changes, $|\rho_{ge}|$ is proportional to ${E_{\rm pump}}^{0.5}$ and $E_{\rm St4}$ is proportional to ${E_{\rm pump}}^{3.4}$. If the energy of the Stokes laser pulses ($E_{\rm Stokes}$) changes, $|\rho_{ge}|$ is proportional to ${E_{\rm Stokes}}^{0.4}$ and $E_{\rm St4}$ is proportional to ${E_{\rm Stokes}}^{3.5}$. The changes of the driving pulse energies correspond to the actual fluctuations of them in the experiments or the change of the overlap between them. Indeed, the fluctuations of both driving pulse energies should contribute to the coherence fluctuation compoundly. From the relative standard deviation of the energy of the fourth Stokes scattering 70%, the fluctuation of the effective energy of the pump laser pulses is estimated to be $+20/-30$%. This corresponds to the coherence fluctuation of $+9/-19$%, while, on the other hand, the fluctuation of the effective energy of the Stokes laser pulses is estimated to be $+20/-30$%. This corresponds to the coherence fluctuation of $+7/-16$%. The asymmetric errors are due to the large variation of the energy of the fourth Stokes scattering.

A theoretical study of the dependence of TPE efficiency on signal frequency has been reported previously, as mentioned in Sec. I. This study is an experimental demonstration of the frequency dependence of coherently amplified TPE over a wide wavelength range of 5.048–10.21 μm.

IV. DISCUSSION

Harris and Jain calculated the parametric gain associated with population-trapped atoms that are prepared with coherence [13]. In their calculation, they assumed that coherence is generated by the driving fields only, and remains constant along the propagation direction. They neglected higher-order Raman sidebands, time dependence of the electric fields, and transverse modes. According to their theoretical calculation, the ratio of TPE signal intensity at position z to the trigger intensity is given as follows:

$$\left|\frac{E_{\rm sig}(z)}{E_{\rm trig}(z=0)}\right|^2=\left|\frac{\kappa_{\rm sig}}{s}\sinh(sz)\right|^2, \tag{1}$$

where

$$s=\left(\kappa_{\rm trig}^{*}\kappa_{\rm sig}-\frac{\Delta k^2}{4}\right)^{1/2}, \tag{2}$$

$$\kappa_{\rm trig(sig)}=\frac{\omega_{\rm trig(sig)}\mathcal{N}}{c}(d_{\rm trig}+d_{\rm sig})|\rho_{ge}|, \tag{3}$$

$$d_{\rm trig(sig)}=\frac{1}{2\hbar\varepsilon_0}\sum_j\frac{d_{gj}d_{je}}{\omega_j-\omega_e+\omega_{\rm trig(sig)}}, \tag{4}$$

$$\Delta k=(k_{\rm pump}-k_{\rm Stokes})-(k_{\rm trig}+k_{\rm sig}). \tag{5}$$

Here, $E_{\rm trig(sig)}(z)$ is the electric field of the trigger (TPE signal) at position z, $\kappa_{\rm trig(sig)}$ is the coupling constant between the trigger and TPE signal fields, and Δk is the **k**-vector mismatch. Furthermore, $\mathcal{N}$ is the number density of p-H_2, c is the speed of light, and ρ_{ge} is the off-diagonal element of the density matrix, which indicates the prepared coherence. Each intermediate level $|j\rangle$ with energy of $\hbar\omega_j$ is coupled to level $|g(v=0)\rangle$ with energy $\hbar\omega_g$ and level $|e(v=1)\rangle$ with energy of $\hbar\omega_e$ by electric dipole transitions, the transition dipole moments of which are represented as d_{gj} and d_{je}. Terms $k_i(i=\text{pump,Stokes,trig,sig})$ are the **k** vectors of the pump, Stokes, trigger, and TPE signal pulses, respectively. Equation (1) indicates that the TPE efficiency as defined by the energy ratio tends to increase with the frequency of the TPE signal, although this increase is accompanied with oscillatory behavior when s is an imaginary number and z is long.

To estimate $d_{\rm trig(sig)}$, the 0−36th vibrational states of the $B\,^1\Sigma_u^+$ state and the 0−13th states of the $C\,^1\Sigma_u$ state are taken into account for the intermediate states $|j\rangle$. The **k**-vector mismatch of Δk is estimated to be 49 $\rm m^{-1}$ at this pressure and temperature, even when the trigger and TPE signal wavelengths change. This is because the refractive index is expected to remain reasonably constant in the midinfrared region. Here we use the dispersion formula for hydrogen gas from Ref. [18]. It was obtained by measuring the refractive indices from 168 nm to 1695 nm. We use the same formula for the trigger and the TPE signal fields by extrapolating it to the midinfrared region because those in the midinfrared region have not been measured so far.

The red solid line in Fig. 5 is the fit of Eq. (1) to the experimental data with the coherence as the only free parameter. This is achieved by an unweighted least-squares fit because the fluctuations of the data points are larger than the displayed error bars determined by the linear fit. The coherence is assumed here to be almost the same at each data point,

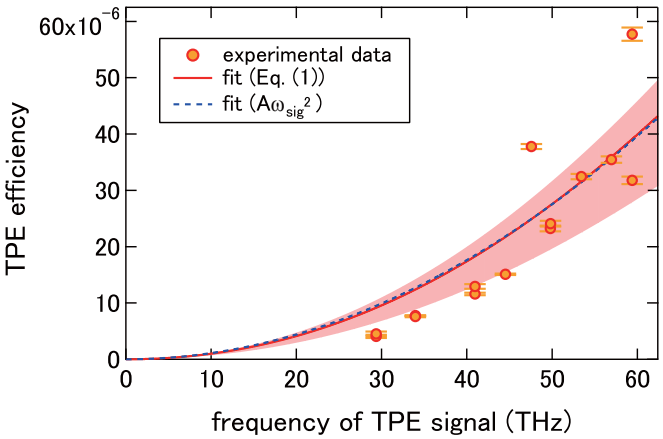

FIG. 5. Experimental data and fit results for the TPE efficiency as defined by the energy ratio as a function of the TPE signal frequency. The orange circles represent the same experimental data as those in Fig. 4(b). The red solid line and the blue dashed line are the fits of Eq. (1) and $A\omega_{sig}^2$, respectively. The shaded area represents a coherence fluctuation of $+7/-16\%$.

although it fluctuates in the experiment. Furthermore, z is set as a target length of 0.15 m. The fitting result gives a coherence of $|\rho_{ge}| = 0.0068$. Considering that the estimated coherence fluctuation is at least $+7/-16\%$, the coherence should lie in the range 0.0058–0.0073. This corresponds to the shaded area in Fig. 5. Both the measured and calculated efficiencies show consistent increases with the frequency of the TPE signal. Furthermore, the measured data points are consistent with the shaded area within the experimental uncertainty. This suggests that the approximation used to derive Eq. (1) is reasonable under the present experimental conditions.

Considering the dependence on TPE signal frequency, Eq. (1) can be reduced to a quadratic function of $\omega_{\rm sig}$ at low coherence. This is because $s \approx \frac{\Delta k}{2} i$ at low coherence and is almost independent of $\omega_{\rm sig}$ because of the nearly constant Δk. Therefore, only $\kappa_{\rm sig}$ has a clear dependence on $\omega_{\rm sig}$ among the variables in Eq. (1). The blue dashed line in Fig. 5 is the unweighted least-squares fit of $A\omega_{\rm sig}^2$ to the data, with A as the free parameter. This line is almost identical to the red line that represents the fit of Eq. (1).

The present study demonstrates the frequency dependence of TPE and suggests a possible application as a broadband wavelength-conversion scheme. To increase the TPE signal energy exponentially along the propagation direction, the parameter s should be a real number. Unfortunately, because Δk is large, even if the coherence were maximized as 0.5, we would still have $s = 20.7i$ (i.e., imaginary) at a pressure of 60 kPa and a temperature of 78 K. Hence the TPE signal energy would not increase exponentially but rather would oscillate sinusoidally. To realize an exponential increase, a small phase mismatch and high coherence are necessary. For example, if $\lambda_{\rm pump} = 1064$ nm and $\lambda_{\rm Stokes} = 1911$ nm are used for a pump and a Stokes laser pulse, respectively, we have $\Delta k = 8.4$–9.1 m^{-1} for $0 < \omega_{\rm sig} < \omega_{\text{p-H}_2}$. Exponential increase is realized at $\omega_{\rm sig}/2\pi = 60$, 30, and 10 THz if the prepared coherence is higher than 0.10, 0.11, and 0.17, respectively. Photons with frequencies less than the difference between the vibrational levels can be generated without any absorption by the medium for the case of p-H_2 by changing the wavelength of the trigger field, such as the THz region.

V. CONCLUSIONS

In summary, we have used the vibrational energy levels of p-H_2 to make measurements of the dependence of the efficiency of coherently amplified TPE on the signal frequency. A quadratic dependence is predicted theoretically in the case of low coherence. The experimental results agree with the theoretical predictions within the experimental uncertainty. This study has demonstrated the frequency dependence of coherently amplified TPE experimentally, and also its potential as a light source. If wavelengths that reduce the phase mismatch are chosen for the driving fields, the exponential increase of the TPE signal can be realized over a wide frequency range if high coherence is prepared.

ACKNOWLEDGMENTS

This work was supported by JSPS KAKENHI (Grants No. JP15H02093, No. JP15H03660, No. JP15K13486, No. JP15K17651, No. JP17K14363, and No. JP17K18779) and JST, PRESTO Grant No. JPMJPR16P3. T.H. acknowledges support from JSPS KAKENHI Grant No. 16J10938.

[1] M. Fleischhauer, A. Imamoglu, and J. P. Marangos, Rev. Mod. Phys. **77**, 633 (2005).
[2] K. Bergmann, H. Theuer, and B. W. Shore, Rev. Mod. Phys. **70**, 1003 (1998).
[3] N. A. Kurnit, I. D. Abella, and S. R. Hartmann, Phys. Rev. Lett. **13**, 567 (1964).
[4] R. H. Dicke, Phys. Rev. **93**, 99 (1954).
[5] D. Meiser, J. Ye, D. R. Carlson, and M. J. Holland, Phys. Rev. Lett. **102**, 163601 (2009).
[6] A. Fukumi, S. Kuma, Y. Miyamoto, K. Nakajima, I. Nakano, H. Nanjo, C. Ohae, N. Sasao, M. Tanaka, T. Taniguchi, S. Uetake, T. Wakabayashi, T. Yamaguchi, A. Yoshimi, and M. Yoshimura, Prog. Theor. Exp. Phys. **2012**, 04D002 (2012).
[7] G. Breit and E. Teller, Astrophys. J. **91**, 215 (1940).
[8] M. Lipeles, R. Novick, and N. Tolk, Phys. Rev. Lett. **15**, 690 (1965).
[9] Y. B. Bannett and I. Freund, Phys. Rev. A **30**, 299 (1984).
[10] J. Schirmer, D. Habs, R. Kroth, N. Kwong, D. Schwalm, M. Zirnbauer, and C. Broude, Phys. Rev. Lett. **53**, 1897 (1984).
[11] P. H. Mokler and R. W. Dunford, Phys. Scr. **69**, C1 (2004).
[12] A. Hayat, P. Ginzburg, and M. Orenstein, Nat. Photon. **2**, 238 (2008).
[13] S. E. Harris and M. Jain, Opt. Lett. **22**, 636 (1997).

[14] Y. Miyamoto, H. Hara, S. Kuma, T. Masuda, I. Nakano, C. Ohae, N. Sasao, M. Tanaka, S. Uetake, A. Yoshimi, K. Yoshimura, and M. Yoshimura, Prog. Theor. Exp. Phys. **2014**, 113C01 (2014).

[15] Y. Miyamoto, H. Hara, T. Masuda, N. Sasao, M. Tanaka, S. Uetake, A. Yoshimi, K. Yoshimura, and M. Yoshimura, Prog. Theor. Exp. Phys. **2015**, 081C01 (2015).

[16] W. K. Bischel and M. J. Dyer, Phys. Rev. A **33**, 3113 (1986).

[17] Y. Miyamoto, H. Hara, T. Masuda, T. Hiraki, N. Sasao, and S. Uetake, Jpn. J. Appl. Phys. **56**, 032101 (2017).

[18] E. R. Peck and S. Huang, J. Opt. Soc. Am. **67**, 1550 (1977).